



ELSEVIER

Journal of Alloys and Compounds 224 (1995) 207–211

Journal of  
ALLOYS  
AND COMPOUNDSCrystal structure and phase transitions in  $\beta$ - $\text{NH}_3(\text{CH}_2)_2\text{NH}_3\text{HPO}_4$ 

S. Chaabouni, S. Kamoun

*Laboratoire de Cristalochimie du Solide, Ecole Nationale d'Ingénieurs de Sfax, 3038, Sfax, Tunisia*

Received 16 November 1994; in final form 17 January 1995

**Abstract**

Chemical preparation and main crystallographic, calorimetric, dielectric and structural features are given for a new monophosphate.  $\beta$ - $\text{NH}_3(\text{CH}_2)_2\text{NH}_3\text{HPO}_4$  salt is monoclinic  $P2_1/c$  with unit cell dimensions  $a = 10.189(2)$ ;  $b = 7.881(1)$ ;  $c = 8.021(1)$  Å;  $\beta = 92.11(1)^\circ$ ;  $Z = 4$ ;  $D_m = 1.604 \text{ Mg m}^{-3}$ ;  $D_x = 1.632 \text{ Mg m}^{-3}$ ;  $\mu = 1.945 \text{ mm}^{-1}$ ;  $F(000) = 336$ ;  $T = 298 \text{ K}$ ;  $R = 0.044$  and  $R_w = 0.047$  for 1773 observed reflexions. The examination of the structure shows a layer arrangement: planes of  $\text{HPO}_4^{2-}$  alternate with planes of  $[(\text{CH}_2)_2(\text{NH}_3)_2]^{2+}$ . These planes are linked together through hydrogen bonds. Physical measurements carried out at high temperature show clearly that the  $\beta$  variety presents calorimetric and dielectric behaviours different from those observed for the  $\alpha$  variety.

**Keywords:** Organic phosphate; Structure; Phase transitions; Dielectric measurement

**1. Introduction**

During a systematic investigation of interaction between monophosphoric acid and ethylene diamine, we generally observed the formation of  $\alpha$ - $\text{NH}_3(\text{CH}_2)_2\text{NH}_3\text{HPO}_4$  [1],  $\text{NH}_3(\text{CH}_2)_2\text{NH}_3(\text{H}_2\text{PO}_4)_2$  [2,3] and  $\text{NH}_3(\text{CH}_2)_2\text{NH}_3(\text{H}_2\text{PO}_4)_2\text{H}_3\text{PO}_4$  [4]. In some cases, the formation of more compounds was observed during the investigation of the  $\text{M}^I_2\text{O}$ -ethylenediamine- $\text{H}_3\text{PO}_4$  system ( $\text{M}^I$  is a monovalent cation). Up to now, only one compound has been reported:  $\text{Na}_2\text{NH}_3(\text{CH}_2)_2\text{NH}_3(\text{HPO}_4)_2 \cdot 6\text{H}_2\text{O}$  [5]. If the latter synthesis is carried out with other monovalent cations ( $\text{M}^I = \text{K}^+$ ,  $\text{NH}_4^+$ ,  $\text{Cs}^+$ ,  $\text{Rb}^+$ ), only two kinds of complex are obtained. The chemical analysis of these compounds shows that they are devoid of monovalent cations: thus they belong to the binary  $\text{H}_3\text{PO}_4$ -ethylenediamine system.

Crystallographic study shows that the ethylenediammonium monohydrogen-monophosphate salts crystallize in the monoclinic system with space groups  $P2_1/c$  for the  $\alpha$  variety [1] and  $P2_1/a$  for the  $\beta$  variety.

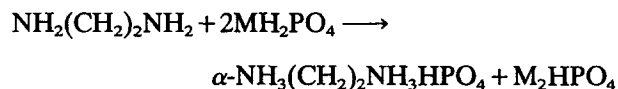
Detailed crystallographic, calorimetric, dielectric and structure features for the  $\beta$  variety are given.

**2. Experimental details****2.1. Crystal chemistry**

The  $\alpha$  and  $\beta$  ethylenediammonium monohydrogen monophosphates are obtained by mixing a solution of

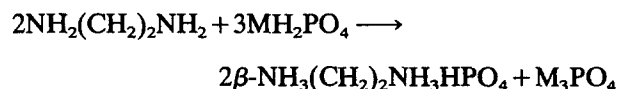
ethylenediamine with an aqueous solution of the monovalent phosphate  $\text{MH}_2\text{PO}_4$ , where  $\text{M}^I = (\text{K}^+, \text{NH}_4^+, \text{Cs}^+, \text{Rb}^+)$ . The chemical reactions are as follows.

If the ratio diamine/ $\text{MH}_2\text{PO}_4 < \frac{1}{2}$  and the  $\text{pH} < 8$ , the  $\alpha$  variety is formed:



with  $\text{M} = \text{K}^+, \text{NH}_4^+, \text{Cs}^+, \text{Rb}^+$ .

If the ratio diamine/ $\text{MH}_2\text{PO}_4 < \frac{3}{2}$  and the  $\text{pH} > 10$ , the  $\beta$  variety is formed:



The resulting aqueous solutions are then kept at room temperature. After some days of evaporation, colorless prism-shaped monocrystals appear in the solution. The chemical analysis of phosphorus and acidic protons has been carried out [6].

Weissenberg and oscillation photographs taken with  $\text{Cu K}\alpha$  radiation show that the  $\beta$ - $\text{NH}_3(\text{CH}_2)_2\text{NH}_3\text{HPO}_4$  salt crystallizes in the monoclinic system with the following unit cell dimensions:

$$a = 10.189(2), b = 7.881(1), c = 8.021(1) \text{ \AA}, \beta = 92.11(1)^\circ$$

The unit cell dimensions were obtained from a least-squares refinement using the data of the diffractograms reported in Table 1. Density was measured at room

Table 1

Indexed powder diagram for  $\beta\text{-NH}_3(\text{CH}_2)_2\text{NH}_3\text{HPO}_4$ . Data have been recorded with a two-circle diffractometer STOE/CSS using cobalt  $K\alpha$  radiation, with a step width 0.04 ( $2\theta$ ) and scan time of 30 s on every step. Intensities reported in this table are relative peaks heights above the background. Unit cell dimensions reported in this work have been refined by a least-squares method using the angular data of this diffractogram

$h k l$	$d_{\text{obs}}$	$d_{\text{cal}}$	$I_{\text{obs}}$	$h k l$	$d_{\text{obs}}$	$d_{\text{cal}}$	$I_{\text{obs}}$
1 1 0	6.23	6.23	19	0 2 3	2.211	2.211	2
0 1 1	5.62	5.62	23	$\bar{1}$ 2 3	2.174	2.175	2
2 0 0	5.09	5.09	13	$\bar{1}$ 3 2	2.156	2.156	16
$\bar{1}$ 1 1	4.97	4.97	36	1 3 2		2.139	
1 1 1	4.87	4.87	39	4 2 0	2.137	2.138	3
0 0 2	4.01	4.01	17	3 2 2		2.137	
0 2 0	3.941	3.941	3	4 0 2	2.114	2.114	2
$\bar{2}$ 1 1	3.823	3.823	100	$\bar{4}$ 1 2	2.106	2.106	3
1 0 2	3.778	3.777	30	4 1 2	2.042	2.042	2
2 1 1	3.726	3.726	86	2 2 3		2.006	
1 0 2	3.684	3.684	34	0 0 4	2.004	2.004	8
0 1 2	3.570	3.572	3	2 3 2		2.003	
0 2 1	3.536	3.536	6	5 1 0	1.970	1.972	4
3 0 0	3.396	3.394	21	0 4 0		1.970	
$\bar{1}$ 2 1	3.358	3.358	56	0 1 4	1.942	1.942	1
1 2 1	3.324	3.324	16	1 4 0	1.930	1.934	5
3 1 0	3.114	3.117	23	$\bar{5}$ 1 1		1.931	
2 2 0		3.116		0 4 1	1.911	1.913	2
2 0 2	3.095	3.094	15	$\bar{4}$ 2 2		1.911	
$\bar{2}$ 1 2	2.971	2.971	1	$\bar{3}$ 2 3		1.879	
$\bar{3}$ 1 1	2.938	2.939	10	1 4 1	1.877	1.877	4
2 2 1	2.881	2.882	7	0 3 3		1.873	
2 1 2		2.880		4 2 2	1.861	1.863	4
0 2 2	2.810	2.810	10	$\bar{3}$ 3 2		1.862	
$\bar{1}$ 2 2	2.727	2.727	2	$\bar{5}$ 0 2	1.842	1.843	8
3 2 0	2.572	2.572	1	2 0 4		1.842	
0 1 3	2.530	2.530	20	3 2 3		1.828	
$\bar{3}$ 1 2	2.502	2.502	11	3 3 2	1.827	1.828	1
$\bar{3}$ 2 1	2.469	2.469	2	4 3 0		1.828	
1 3 1	2.419	2.418	11	$\bar{4}$ 1 3		1.827	
$\bar{4}$ 1 1	2.341	2.342	3	5 2 0	1.809	1.809	2
$\bar{2}$ 1 3	2.296	2.298	4				
4 1 1		2.297					

temperature by flotation in bromobenzene. The average value of density,  $D_m = 1.604 \text{ Mg m}^{-3}$ , is in agreement with that calculated,  $D_x = 1.632 \text{ Mg m}^{-3}$ . The cell contains four formula units of  $\beta\text{-NH}_3(\text{CH}_2)_2\text{NH}_3\text{HPO}_4$ . Indexed powder data are given in Table 1.

## 2.2. Crystal structure determination

Experimental conditions used for the single crystal diffraction data collections are reported in Table 2. Lorentz and polarization corrections have been made but an absorption correction was not applied because of the penetrating power of Ag  $K\alpha$  radiation. The crystal structure has been solved using classical methods: interpretation of the three-dimensional Patterson function followed by successive Fourier syntheses. After introducing anisotropic thermal factors for the non-

hydrogen atoms and isotropic ones for H atoms, the final refinement cycles with 1773 reflexions corresponding to  $|F_o - F_c| > 1\sigma_F$  yield  $R = 0.044$ ,  $R_w = 0.047$ ,  $S = 0.753$ . The maximal residual electron density is  $0.427 \text{ e \AA}^{-3}$ . Scattering factors and the anomalous dispersion factors were taken from the *International Tables for X-Ray Crystallography* [7]. Enraf Nonius SDP was employed for all refinements [8].

## 3. Results and discussion

### 3.1. Description of the structure

The final atomic coordinates and  $B_{\text{eq}}$  or  $B_{\text{iso}}$  are given in Table 3. Interatomic distances, bond angles and the hydrogen bonds are given in Table 4. Anisotropic

Table 2  
Experimental conditions used during the intensity data collection

Apparatus	Philips PW 1100
Monochromator	Graphite plate
Wavelength	0.5608 (Ag K $\alpha$ )
Scan mode	$\omega$
Scan speed ( $^{\circ}$ s $^{-1}$ )	0.02
Total background measurements (s)	10
Scan width ( $^{\circ}$ )	1 + 0.2 tan $\theta$
Theta range ( $^{\circ}$ )	3 to 30
Intensity reference reflexions	$\bar{1}32, \bar{1}\bar{3}2, 13\bar{2}$
Number of collected reflexions	1792 ( $\pm h, k, l$ )
Crystal size (mm)	0.1 $\times$ 0.14 $\times$ 0.12
$h_{\max}, k_{\max}, l_{\max}$	18, 13, 7

Table 3  
Atomic coordinates and  $B_{\text{eq}}$  or  $\beta_{\text{iso}}$  for  $\beta$ -NH $_3$ (CH $_2$ ) $_2$ NH $_3$ HPO $_4$

$$B_{\text{eq}} = \frac{4}{3} \sum_i \sum_j a_i a_j \beta_{ij}$$

Atoms	X( $\sigma$ )	Y( $\sigma$ )	Z( $\sigma$ )	$B_{\text{eq}}(\sigma)/\beta_{\text{iso}}(\sigma)$
P	0.25270(6)	0.06974(8)	0.39982(8)	1.428(7)
O(1)	0.3035(3)	0.4347(3)	0.0891(2)	3.00(4)
O(2)	0.2679(2)	0.8846(2)	0.3461(2)	1.74(3)
O(3)	0.1105(2)	0.375(3)	0.8896(2)	2.39(3)
O(4)	0.3398(2)	0.1866(2)	0.3030(3)	2.50(3)
N(1)	0.9674(2)	0.2944(3)	0.6097(3)	1.92(3)
N(2)	0.4207(2)	0.8017(3)	0.0779(3)	1.76(3)
C(2)	0.4440(2)	0.5523(3)	0.4666(3)	2.04(4)
H(O1)	0.298(3)	0.148(5)	0.652(5)	1.6(7)*
H(1N1)	0.018(3)	0.276(4)	0.046(4)	2.0(6)*
H(2N1)	0.985(3)	0.683(4)	0.296(4)	3.1(7)*
H(3N1)	0.107(3)	0.767(4)	0.365(4)	2.3(6)*
H(1N2)	0.499(3)	0.715(5)	0.605(4)	3.6(7)*
H(2N2)	0.371(3)	0.719(4)	0.023(4)	2.6(7)*
H(3N2)	0.372(3)	0.661(4)	0.665(4)	3.7(8)*
H(1C1)	0.115(3)	0.028(4)	0.906(4)	1.9(6)*
H(2C1)	0.126(3)	0.936(4)	0.073(4)	2.9(7)*
H(1C2)	0.359(3)	0.010(4)	0.954(4)	3.2(7)*
H(2C2)	0.538(4)	0.097(5)	0.146(5)	4.6(9)*

\* ( $\beta$ ): isotropic.

thermal parameters for the non-hydrogen atoms are reported in Table 5. The projection along the  $\bar{c}$  axis of the atomic arrangement of the  $\beta$  variety is depicted in Fig. 1. An examination of the structure clearly shows a layer arrangement: planes of HPO $_4^{2-}$  tetrahedra alternate with planes of [(CH $_2$ ) $_2$ (NH $_3$ ) $_2$ ] $^{2+}$  groups. The HPO $_4^{2-}$  tetrahedra are associated in pairs forming centrosymmetric finite clusters, [H $_2$ P $_2$ O $_8$ ] $^{4-}$ . The P–P distance between two HPO $_4$  groups linked by two hydrogen bonds is 4.931(1) Å. The P–O distances range from 1.517(2) to 1.592(2) Å. The longest P–O distance, 1.592(2) Å, is due to the presence of the acidic hydrogen atom on the PO $_4$  tetrahedron.

Table 4  
Principal interatomic distances (Å) and bond angles ( $^{\circ}$ ) and details of the hydrogen bonding scheme

PO $_4$  tetrahedron:

P	O(1)	O(2)	O(3)	O(4)
O(1)	<u>1.592(2)</u>	102.5(1)	109.7(1)	109.1(1)
O(2)	2.439(3)	<u>1.535(2)</u>	111.4(2)	111.6(1)
O(3)	2.543(3)	2.522(3)	<u>1.517(2)</u>	112.1(1)
O(4)	2.533(3)	2.525(3)	2.517(3)	<u>1.517(2)</u>

P–P: 4.931(1) Å  
O(1)–H(O1): 0.83(4) Å  
P–O(1)–H(O1): 123(3) $^{\circ}$

[NH $_3$ (CH $_2$ ) $_2$ NH $_3$ ] $^{2+}$  group:

N(1)–H(1N1): 0.92(3)	H(1N1)–N(1)–H(2N1): 106.8(2)
N(1)–H(2N1): 0.91(3)	H(1N1)–N(1)–H(3N1): 106.5(2)
N(1)–H(3N1): 0.93(3)	H(2N1)–N(1)–H(3N1): 109.8(2)
N(2)–H(1N2): 0.92(3)	H(1N2)–N(2)–H(2N2): 121.1(2)
N(2)–H(2N2): 0.93(3)	H(1N2)–N(2)–H(3N2): 113.1(2)
N(2)–H(3N1): 0.92(4)	H(2N2)–N(2)–H(3N2): 106.6(2)
C(1)–H(1C1): 0.96(3)	H(1C1)–C(1)–H(2C1): 101.2(2)
C(1)–H(2C1): 1.01(3)	
C(2)–H(1C2): 1.00(3)	H(1C2)–C(2)–H(2C2): 105.8(2)
C(2)–H(2C2): 0.99(4)	
N(1)–C(1): 1.479(3)	N(1)–C(1)–C(1): 110.2(2)
N(2)–C(2): 1.486(3)	N(2)–C(2)–C(2): 110.5(2)

Hydrogen bonds:

	O(N)–H	H...O(N)	O(N)...O	O(N)H...O
O(1)–H(O1)...O(4)	0.83(4)	1.82(4)	2.627(3)	163(4)
N(1)–H(1N1)...O(3)	0.92(3)	1.79(3)	2.694(3)	167(3)
N(1)–H(2N1)...O(3)	0.91(3)	1.81(3)	2.718(3)	177(3)
N(1)–H(3N1)...O(2)	0.93(3)	1.90(3)	2.825(3)	171(3)
N(2)–H(1N2)...O(4)	0.92(3)	1.85(3)	2.753(3)	166(3)
N(2)–H(2N2)...O(2)	0.93(3)	1.92(3)	2.808(3)	158(3)
N(2)–H(3N2)...O(2)	0.92(43)	1.87(3)	2.786(3)	173(3)

Table 5  
Anisotropic thermal parameters ( $\times 10^3$ ) for  $\beta$ -NH $_3$ (CH $_2$ ) $_2$ NH $_3$ HPO $_4$ . The temperature factor used here is:  
 $T = \exp[-(\beta_{11}h^2 + \beta_{22}k^2 + \beta_{33}l^2 + 2\beta_{12}hk + 2\beta_{13}hl + 2\beta_{23}kl)]$

Atoms	$\beta_{11}$	$\beta_{22}$	$\beta_{33}$	$\beta_{12}$	$\beta_{13}$	$\beta_{23}$
P	1.63(1)	1.28(1)	1.37(1)	0.07(2)	−0.18(1)	−0.01(2)
O(1)	4.86(9)	2.33(7)	1.71(6)	−0.91(8)	−1.15(6)	0.26(6)
O(2)	2.01(6)	1.43(5)	1.77(6)	0.10(5)	0.05(5)	0.19(5)
O(3)	2.04(6)	2.96(7)	2.19(7)	−0.84(6)	0.20(6)	0.06(6)
O(4)	2.33(6)	2.21(6)	2.93(7)	−0.64(6)	−0.33(6)	0.92(6)
N(1)	2.01(7)	1.85(7)	1.92(7)	−0.31(6)	0.25(6)	−0.00(6)
N(2)	1.79(6)	1.65(6)	1.87(6)	−0.13(6)	0.21(6)	−0.07(6)
C(1)	1.66(7)	1.94(9)	2.43(9)	−0.02(6)	0.06(7)	0.19(7)
C(2)	2.20(7)	2.12(9)	1.77(7)	0.62(7)	−0.37(6)	−0.30(7)

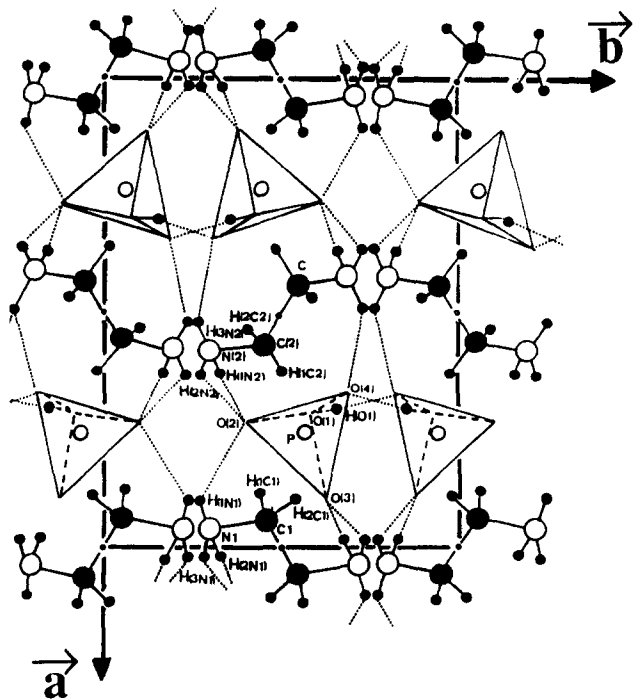
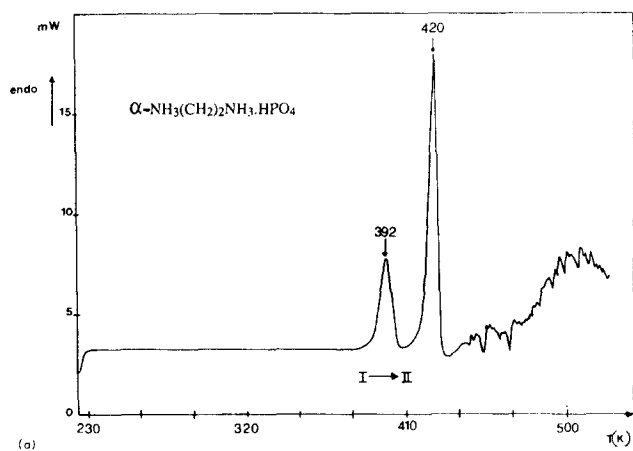
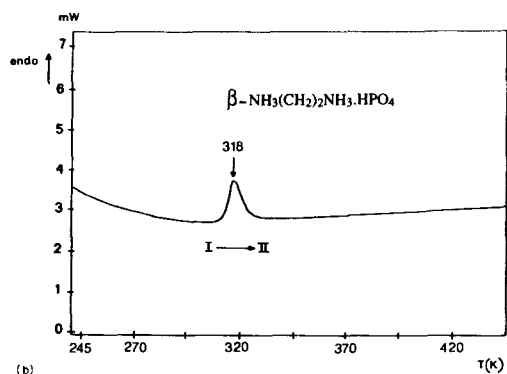


Fig. 1. Projection along the  $\bar{c}$  axis of the atomic arrangements of  $\beta$ - $\text{NH}_3(\text{CH}_2)_2\text{NH}_3\text{HPO}_4$ .

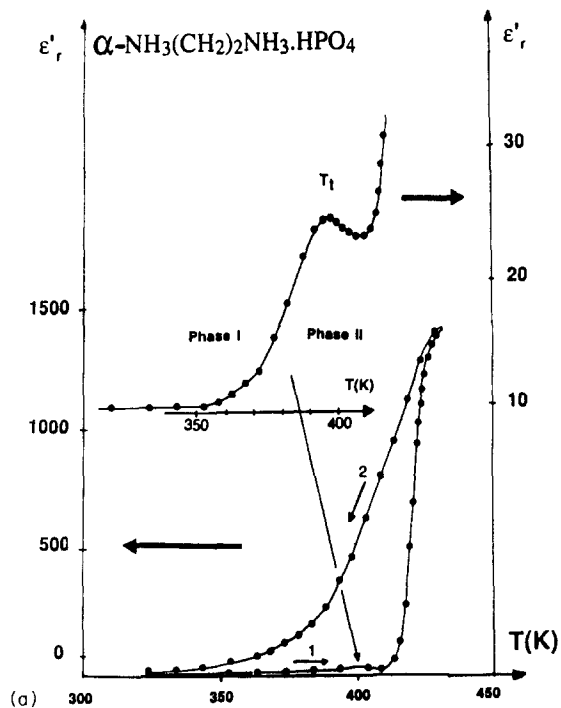


(a)

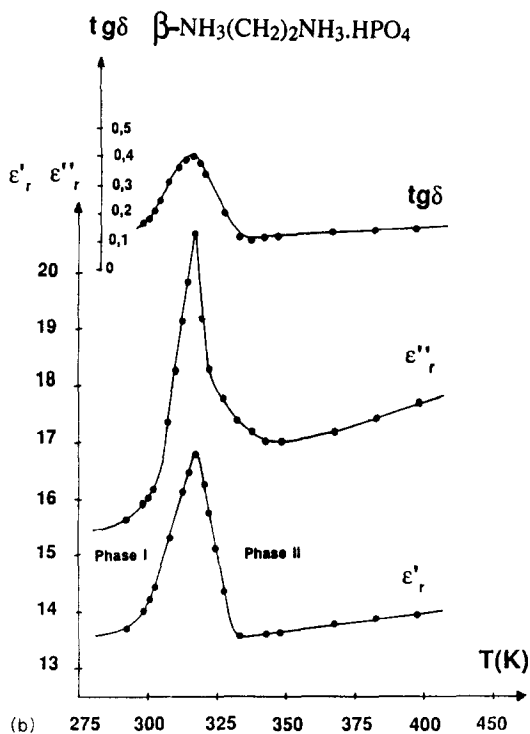


(b)

Fig. 2. (a) Differential scanning calorimeter run on  $\alpha$ - $\text{NH}_3(\text{CH}_2)_2\text{NH}_3\text{HPO}_4$ . (b) Differential scanning calorimeter run on  $\beta$ - $\text{NH}_3(\text{CH}_2)_2\text{NH}_3\text{HPO}_4$ .



(a)



(b)

Fig. 3. (a) Thermal variation of  $\epsilon'_{r[0,k,0]}$  for crystal of  $\alpha$ - $\text{NH}_3(\text{CH}_2)_2\text{NH}_3\text{HPO}_4$  salt. (b) Thermal variation of  $\epsilon'_{r[0,k,0]}$  for crystal of  $\beta$ - $\text{NH}_3(\text{CH}_2)_2\text{NH}_3\text{HPO}_4$ .

The organic groups, present as a dication  $[(\text{CH}_2)_2(\text{NH}_3)_2]^{2+}$ , are centrosymmetric in the  $\beta$  variety and strongly pseudo-symmetric in the  $\alpha$  variety [1]. Table 4 reports the principal geometrical features of the  $[(\text{CH}_2)_2(\text{NH}_3)_2]^{2+}$  groups.

The intermolecular hydrogen bonding contacts of the type N-H...O provide a linkage between cationic entities

$[(\text{CH}_2)_2(\text{NH}_3)_2]^{2+}$  and  $[\text{H}_2\text{P}_2\text{O}_8]^{4-}$  anionic clusters. All the hydrogen bonds (O–H...O and N–H...O types) give rise to a three-dimensional network in the structure and add stability to this compound.

### 3.2. Phase transition in $\alpha$ - and $\beta$ - $\text{NH}_3(\text{CH}_2)_2\text{-NH}_3\text{HPO}_4$

Differential scanning calorimetry (DSC) experiments were performed on heating  $\alpha$ - and  $\beta$ -ethylenediammonium monohydrogen monophosphate samples from 300 K to 440 K. The thermal analysis results are reported in Figs. 2(a) and 2(b).

For the  $\alpha$  variety, the thermogram shows two endothermic peaks at  $T_1=392$  K and  $T_2=420$  K (Fig. 2(a)). The enthalpy and entropy changes are respectively  $\Delta H_1=7.11$  kJ mol<sup>-1</sup> and  $\Delta S_1=18.15$  J mol<sup>-1</sup> K<sup>-1</sup>. The first transition observed at 392 K is reversible. For this transition, the relation  $\Delta S=R \ln\Omega$  brings to a number of equivalent positions  $\Omega=8.87$ ; this value means that the relative disorder of the high-temperature phase is of a complex nature, and probably reflects a conformational modification of organic chains rather than a statical distribution of atoms between different positions. The second transition observed at 420 K corresponds to the melting of the  $\alpha$  variety. The melting enthalpy and entropy are respectively  $\Delta H_2=17.57$  kJ mol<sup>-1</sup> and  $\Delta S_2=41.84$  J mol<sup>-1</sup> K<sup>-1</sup>.

For the  $\beta$  variety, the thermogram shows only one endothermic peak at 318 K (Fig. 2(b)). This irreversible transition may be considered to be of the first-order type. The enthalpy and entropy changes are respectively  $\Delta H_1=0.69$  kJ mol<sup>-1</sup> and  $\Delta S_1=2.16$  J mol<sup>-1</sup> K<sup>-1</sup>. The number of equivalent positions is  $\Omega=1.30$ .

#### 3.2.2. Dielectric study

In order to gain more information on the crystal dynamics (short interaction distance), we have under-

taken a dielectric study between 300 and 400 K. The dielectric measurements have been performed at 1 kHz frequency in a nitrogen atmosphere. Single crystals have been oriented by X-ray diffraction. Silver electrodes are laid down via a lacquer put on the faces perpendicular to the  $[0,k,0]$  directions related to the monoclinic cell. Fig. 3(a)–3(b) show respectively the thermal variations of both the permittivity  $\epsilon'_r$  and the dielectric losses  $\tan\delta$  for the  $\alpha$  and  $\beta$  varieties. One maximum of  $\epsilon'_{r[0,k,0]}$  appears at  $(398+2)$  K for the  $\alpha$  variety and at  $(319+2)$  K for the  $\beta$  variety. A maximum of  $\epsilon'_r$ , corresponding to a maximum of  $\tan\delta$  is observed for each sample. This dielectric behaviour rules out the existence of a ferroelectric phase at the high temperature. According to previous studies on this family of compounds [9], it was established that the rotational jumps of  $\text{NH}_3$  groups and the conformational disorder of the aliphatic chains were responsible for the order–disorder transitions.

### References

- [1] M.T. Averbuch-Pouchot and A. Durif, *Acta Crystallogr.*, C43 (1987) 1894.
- [2] S. Kamoun, M. Kamoun, A. Jouini and A. Daoud, *C.R. Acad. Sci. Paris*, T307, Série II (1988) 1761.
- [3] S. Kamoun, M. Kamoun, A. Jouini and A. Daoud, *Acta Crystallogr.*, C45 (1989) 481.
- [4] M. Bagieu-Beucher, A. Durif and J.C. Guitel, *Acta Crystallogr.*, C45 (1989) 421.
- [5] M.T. Averbuch-Pouchot and A. Durif, *Acta Crystallogr.*, C43 (1987) 1996.
- [6] G. Charlot, *Chimie Analytique Quantitative*, Vol. II, Masson et Cie, Paris, 1974.
- [7] *International Tables for X-Ray Crystallography*, Vol. IV, Kynoch Press, Birmingham; 1974.
- [8] Enraf-Nonius, Structure Determination Package, Enraf Nonius Delft, The Netherlands, 1980.
- [9] S. Kamoun, A. Daoud, R. Von der Muhl and J. Ravez, *Solid State Commun.*, 85 (1993) 661.